

Landau levels in curved space realized in strained graphene

Glenn Wagner¹, Fernando de Juan^{2,3}, Dung X. Nguyen^{4,*}

1 Rudolf Peierls Centre for Theoretical Physics, Parks Road, Oxford, OX1 3PU, UK

2 Donostia International Physics Center, Paseo Manuel de Lardizabal, 4, 20018 San Sebastian, Spain

3 IKERBASQUE, Basque Foundation for Science, Maria Diaz de Haro 3, 48013 Bilbao, Spain

4 Brown Theoretical Physics Center and Department of Physics, Brown University, 182 Hope Street, Providence, RI 02912, USA

* dungmuop@gmail.com

November 17, 2020

Abstract

The quantum Hall effect in curved space has been the subject of many theoretical investigations in the past, but devising a physical system to observe this effect is hard. Many works have indicated that electronic excitations in strained graphene realize Dirac fermions in curved space in the presence of a background pseudo-gauge field, providing an ideal playground for this. However, the absence of a direct matching between a numerical, strained tight-binding calculation of an observable and the corresponding curved space prediction has hindered realistic predictions. In this work, we provide this matching by deriving the low-energy Hamiltonian from the tight-binding model analytically to second order in the strain and mapping it to the curved-space Dirac equation. Using a strain profile that produces a constant pseudo-magnetic field and a constant curvature, we compute the Landau level spectrum with real-space numerical tight-binding calculations and find excellent agreement with the prediction of the quantum Hall effect in curved space. We conclude discussing experimental schemes for measuring this effect.

Contents

1	Introduction	2
2	2 + 1D Dirac Fermion in static curved space	3
2.1	Vielbein formalism	4
2.2	2 + 1D Dirac fermion in static curved space	4
3	Deriving the Dirac Hamiltonian from the tight-binding model	6
3.1	Tight-binding Hamiltonian	6
3.2	Mapping to Dirac fermion in static curved space	7

4	Second-order calculation	8
5	Numerical calculation	9
6	Comparison to previous work	10
7	Conclusions	10
A	2 + 1D Dirac fermion in static curved space	12
A.1	Action in curved space-time	12
A.2	Hamiltonian in static curved space	13
B	Derivation of effective tight-binding Hamiltonian	14
B.1	Expansion around the \mathbf{K} point	15
B.2	Expansion around the \mathbf{K}' point	16
B.3	Valley dual transformation	16
C	Which \mathbf{K} point should one expand about?	17
D	Uniform dilatation	18
E	Second-order calculation: linear tunneling	19
F	Second-order calculation: exponential tunneling	20
	References	22

1 Introduction

In the ever-growing field of graphene research, an interesting question is what happens when strain is applied to a sheet of graphene. The answer turns out to be particularly interesting from a theoretical point of view: The particles behave as though they feel an effective magnetic field and are moving in a curved space-time [1–9]. This makes strained graphene a playground for quantum field theory in curved space-time. It is also interesting from a more down-to-Earth materials perspective, leading to the term *straintronics* being coined [10].

The atoms in graphene form a hexagonal lattice. Electrons hopping on this lattice can be described by a simple tight-binding (TB) model [11]. It is a textbook exercise to derive the action for a Dirac fermion by taking the continuum limit of the tight-binding Hamiltonian for graphene [12]. The problem becomes more interesting, once strain is applied, such that neighbouring atoms are displaced by different amounts from their equilibrium position. This will lead to a spatial variation of the hopping strength across the lattice. It can be shown [1–5] that this leads to two corrections to the Dirac action. Firstly, the Dirac fermion is now coupled to an emergent gauge field. Since applying a strain cannot break time-reversal symmetry, the magnetic field derived from the emergent gauge field must have opposite signs at the two Dirac points. Hence it is often referred to as a pseudo-magnetic field. Secondly, the Fermi-velocity

becomes a space-dependent tensor. This can equally be interpreted as a vielbein—the Dirac fermion becomes coupled to curved space. The extra terms can also be derived from general symmetry considerations [13–15].

In our work we derive the mapping between the tight-binding model of strained graphene and the field theory of a Dirac fermion coupled to a gauge field in curved space. We derive the expressions for the gauge field and the vielbein to all orders in the strain. We discuss whether a spin-connection term should appear in the field theory description.

It is possible to engineer a strain profile, such that the emergent gauge field corresponds to a constant magnetic field. In that case, we expect Landau levels (LL) to form and indeed this has been seen in tight-binding calculations [16, 17] and in experiment [18–21]. For the given strain profile, we show that at second order, we obtain a correction to the emergent magnetic field and we also find a constant curvature. We emphasize that in our case this curvature is an effective curvature coming purely from the in-plane strain, in contrast to previous work considering physically curving the graphene sheet [22]. Previous works have also looked at the effect of curvature in fullerenes [23] and carbon nanoribbons [24, 25] as well as the curvature due to topological defects [26, 27].

Previous work that has appeared on strained graphene has tended to focus on the first order in strain [1, 2, 28]. As opposed to other works that have included second order corrections [5, 29], we consider not only the emergent gauge field, but also the resulting curvature. We note that many previous papers have neglected terms that we include in our work, all of which is derived carefully in the appendices.

We perform a numerical tight-binding calculation in which the shift of the Landau levels due to the curvature is clearly seen. In this calculation we see more than 25 Landau levels and their positions match accurately the prediction from the field theory calculation. This provides further support for the field theory we have derived.

Besides the potential experimental realization in solid state graphene, we propose that such a strain profile can be engineered—and the effects of curvature seen—in graphene analogues such as photonic or sonic lattices, where the level of control is much higher than in conventional graphene. In these systems it is possible to modify the position of each lattice site individually. It would be exciting indeed to see the effects of curvature on the quantum Hall effect in these experimental set-ups. Synthetic LL for photons have already been seen in optical resonators [30, 31].

The structure of our paper is the following: In section 2 we introduce the field theory formalism of a Dirac fermion in curved space. We discuss why this implies that there is no spin connection term in the Hamiltonian derived from the TB model. The section 3 shows the explicit map between the continuum Hamiltonian derived from the TB model and the field theory from section 2. We then focus on a particular strain profile for section 4 and use the expressions from section 3 to evaluate the magnetic field and curvature to second order in strain for this particular profile. We perform numerics on this TB model in section 5 and see explicitly the effects of curvature in the results.

2 $2 + 1D$ Dirac Fermion in static curved space

In this section, we will review the general form of the Hamiltonian of a $2 + 1D$ Dirac fermion in static curved space following the textbook by Bertlmann [32]. It can be seen that we do

not have any term corresponding to the spin connection explicitly.

2.1 Vielbein formalism

Let us first introduce some notation that will be useful later on. In particular, we use the vielbein formalism of General Relativity [33, 34], which exploits the fact that there is always a coordinate transformation to a locally flat frame. In our work we choose to focus on the case where the atoms in the graphene sheet only experience in-plane displacements and hence we end up with a $2 + 1D$ problem. The metric of static curved space is given by

$$g_{\mu\nu}(\mathbf{x}) = \begin{pmatrix} 1 & 0 \\ 0 & -g_{ij}(\mathbf{x}) \end{pmatrix}, \quad (2.1)$$

where $i, j, k = 1, 2$ represent the space indices. The flat space-time metric is $\eta_{\alpha\beta} = \text{diag}(1, -1, -1)$. We will use $\alpha, \beta, \gamma, \dots$ for local frame indices and μ, ν, λ, \dots for coordinate indices. We will also use $a, b, c, \dots = 1, 2$ for space indices of the local frame and $i, j, k, \dots = 1, 2$ for space indices of the coordinates. The vielbein is given by the definition $g_{\mu\nu} = e_{\mu}^{\alpha} e_{\nu}^{\beta} \eta_{\alpha\beta}$. We raise and lower the local frame indices by $\eta_{\alpha\beta}$ and $\eta^{\alpha\beta}$, we raise and lower the space coordinate indices by $g_{\mu\nu}$ and $g^{\mu\nu}$. We also define the inverse vielbein e_{α}^{μ} as $e_{\mu}^{\alpha} e_{\beta}^{\mu} = \delta_{\beta}^{\alpha}$. For static curved space, we have

$$e_0^0 = 1, e_0^i = e_a^0 = 0, \quad (2.2)$$

and all the components of the vielbein are time-independent. The spin connection is ¹

$$\omega_{\mu\beta}^{\alpha} = -e_{\beta}^{\nu} (\partial_{\mu} e_{\nu}^{\alpha} - \Gamma_{\mu\nu}^{\sigma} e_{\sigma}^{\alpha}). \quad (2.3)$$

where $\Gamma_{\lambda\sigma}^{\mu}$ is the Christoffel symbol. With the tetrad postulate [33]

$$\nabla_{\mu} e_{\nu}^{\alpha} = \partial_{\mu} e_{\nu}^{\alpha} - \Gamma_{\mu\nu}^{\sigma} e_{\sigma}^{\alpha} + \omega_{\mu\beta}^{\alpha} e_{\nu}^{\beta} = 0, \quad (2.4)$$

we find that the Christoffel symbol in terms of the vielbein is $\Gamma_{\lambda\sigma}^{\mu} = \partial_{\sigma} (e_{\lambda}^{\alpha}) e_{\alpha}^{\mu}$. We also use the explicit notation of gamma matrices with local frame index γ^{α} in $2 + 1D$ as

$$\gamma^0 = \sigma^3, \quad \gamma^a = \sigma^3 \sigma^a \quad (a = 1, 2), \quad (2.5)$$

where σ^a are the Pauli matrices. We have the anti-commutation relation $\{\gamma^a, \gamma^b\} = 2\eta^{ab}I$. The space-dependent gamma matrices with space-time indices are given by

$$\gamma^{\mu}(\mathbf{x}) = e_{\alpha}^{\mu}(\mathbf{x}) \gamma^{\alpha} \quad (2.6)$$

with the anti-commutation relation $\{\gamma^{\mu}(\mathbf{x}), \gamma^{\nu}(\mathbf{x})\} = 2g^{\mu\nu}(\mathbf{x})I$.

2.2 $2 + 1D$ Dirac fermion in static curved space

We recall the action of a spin- $\frac{1}{2}$ Dirac fermion in $2 + 1D$ curved space-time [32–35]

$$\mathcal{S} = i \int d^3x \sqrt{|g|} \bar{\Psi} \gamma^{\mu} (\partial_{\mu} - iA_{\mu} - \frac{i}{2} \omega_{\mu}^{\alpha\beta} \sigma_{\alpha\beta}) \Psi \quad (2.7)$$

¹We consider torsionless spin connection.

where we used $\sigma_{\alpha\beta} = \frac{i}{4} [\gamma_\alpha, \gamma_\beta]$, and $g = \det(g_{\mu\nu})$, and $\bar{\Psi} = \Psi^\dagger \gamma^0$. $\omega_\mu^{\alpha\beta}$ is the spin connection. We see that the action (2.7) isn't real, which implies that the corresponding Hamiltonian isn't Hermitian. However, the tight-binding Hamiltonian (3.1) is explicitly Hermitian and therefore, the action has to be real. Therefore, in order to compare the TB and field theory descriptions, we will use the real action by the following definition [32]

$$\mathcal{S}' = \frac{1}{2} (\mathcal{S} + \mathcal{S}^\dagger). \quad (2.8)$$

It can be shown (see Appendix A) that \mathcal{S} and \mathcal{S}' only differ by a total derivative and are hence equivalent physically. This means that the action (2.7) is pseudo-real with a corresponding pseudo-Hermitian Hamiltonian. In a static curved space (2.1), the Hermitian Hamiltonian corresponding to (2.8) is

$$H = -iv_F \int d^2\mathbf{x} \sqrt{\hat{g}} \left[\Psi^\dagger e_a^i \sigma^a \left(\overleftrightarrow{\partial}_i - iA_i \right) \Psi \right], \quad (2.9)$$

where $\overleftrightarrow{\partial}_\mu = \frac{1}{2} \left(\overrightarrow{\partial}_\mu - \overleftarrow{\partial}_\mu \right)$ only acts on fermion fields. One observes that there is no spin connection term in (2.9) for a static curved metric (2.1). Note that this only works in 2 + 1D [32]. We have inserted the Fermi velocity v_F as appropriate for graphene, and $\hat{g}(\mathbf{x}) = \det(g_{ij}(\mathbf{x}))$. Furthermore, we have set the scalar potential to zero as is appropriate for the type of strain that we consider in this work. We leave the detailed derivation of equation (2.9) to Appendix A.

The inner product of the wave function in static curved space is given by

$$\langle \Phi | \Psi \rangle = \int d^2x \sqrt{\hat{g}} \Phi^\dagger \Psi. \quad (2.10)$$

However, to make a comparison with the tight binding model we need to define a new field

$$\tilde{\Psi} = \hat{g}^{1/4} \Psi, \quad (2.11)$$

with the corresponding wave function's inner product

$$\langle \tilde{\Phi} | \tilde{\Psi} \rangle = \int d^2x \tilde{\Phi}^\dagger \tilde{\Psi}, \quad (2.12)$$

since this inner product is the one that is inherited from the tight-binding model. The Hamiltonian in static curved space has the new form

$$\tilde{H} = -iv_F \int d^2x \tilde{\Psi}^\dagger e_a^i \sigma^a \left(\overleftrightarrow{\partial}_i - iA_i \right) \tilde{\Psi}. \quad (2.13)$$

In the subsequent sections, we will derive the same Hamiltonian (2.13) from strained graphene. Naturally, the inner product of the electron's wave function in graphene takes the form (2.12). It is clear from equation (2.13) that the Hermitian Hamiltonian in static curved space doesn't have the spin connection contribution. However, the equation of motion for the Hermitian Hamiltonian (2.13) has an additional term which includes the derivative of the vielbein. This term originates from the spin connection. See Appendix A for more details.

So in conclusion, in order to compare to the tight-binding Hamiltonian, one has to use the Hermitian Hamiltonian (2.13) instead of the Hamiltonian derived directly from (2.7). There is no explicit spin connection term in (2.13).

3 Deriving the Dirac Hamiltonian from the tight-binding model

3.1 Tight-binding Hamiltonian

Under applied strain, the tunneling parameter in the tight binding (TB) model of graphene depends on the coordinates. We write the TB Hamiltonian in the following form

$$H^{TB} = \sum_{n, \mathbf{R}_i} t_n(\mathbf{R}_i) \left(\psi_A^\dagger(\mathbf{R}_i) \psi_B(\mathbf{R}_i + \mathbf{l}_n) + h.c. \right), \quad (3.1)$$

where $t_n(\mathbf{x})$ is the space dependent tunneling parameter, $\psi_A^\dagger(\mathbf{R}_i)$ is the operator that creates an electron at position \mathbf{R}_i of sub-lattice A and $\psi_B(\mathbf{R}_i + \mathbf{l}_n)$ is the operator that annihilates an electron at position $\mathbf{R}_i + \mathbf{l}_n$ of sub-lattice B . \mathbf{l}_n are vectors from an A site to its nearest neighbours, $\mathbf{l}_1 = a(\frac{\sqrt{3}}{2}, \frac{1}{2})$, $\mathbf{l}_2 = a(-\frac{\sqrt{3}}{2}, \frac{1}{2})$ and $\mathbf{l}_3 = a(0, -1)$.

We Fourier transform the Hamiltonian (3.1) and expand for momenta close to the Dirac point $\mathbf{K} = (\frac{4\pi}{3\sqrt{3}a}, 0)$. We note that there has been some controversy in the literature about whether to expand the Hamiltonian about the unshifted Dirac point \mathbf{K} (as we do here) or about a shifted Dirac point, defined as the point in k -space where the Hamiltonian vanishes. However, following through the expansion around the shifted \mathbf{K} point in the formalism, in Appendix C one encounters divergences when attempting to Fourier transform back to real space, showing that this expansion is inconsistent. See Appendix C for details.

We expand to linear order in the momenta and to all orders in the strain for now. Going back to position space, we can rewrite the Hamiltonian as

$$H^{TB} = \int d^2\mathbf{x} v_F \psi^\dagger(\mathbf{x}) \left(-i\sigma_i \tilde{v}^{ij}(\mathbf{x}) \overleftrightarrow{\partial}_j - \sigma^i A_i^s(\mathbf{x}) \right) \psi(\mathbf{x}) \quad (3.2)$$

with $v_F = \frac{3t_0}{2a}$ and the space dependent Fermi velocity is

$$\tilde{v}^{ij}(\mathbf{x}) = \sum_n \frac{2}{3t_0 a^2} l_n^i l_n^j \left(t_n(\mathbf{x}) - \frac{1}{2} l_n^k \partial_k t_n(\mathbf{x}) \right), \quad (3.3)$$

and the artificial gauge field due to the strain is given by

$$A_i^s(\mathbf{x}) = \sum_n \frac{2}{3t_0 a^2} \epsilon_{ij} l_n^j \left(t_n(\mathbf{x}) - \frac{1}{2} l_n^k \partial_k t_n(\mathbf{x}) \right) \quad (3.4)$$

and $\psi(\mathbf{x})$ is a Dirac spinor with the spinor index corresponding to the sub-lattice index

$$\psi(\mathbf{x}) = e^{i\mathbf{K}\cdot\mathbf{x}} \begin{pmatrix} \psi_A(\mathbf{x}) \\ \psi_B(\mathbf{x}) \end{pmatrix}. \quad (3.5)$$

The technical details of this calculation are left to the Appendix B. The result (3.2) together with (3.3) and (3.4) are central results of this work. The last term of (3.3) and (3.4) was missed in the previous works [1, 2]. Furthermore, we can show that there is a symmetry operation relating the low-energy theory around \mathbf{K} and around the other Dirac point $\mathbf{K}' = -\mathbf{K}$, such that the spectra are the same (see Appendix B for details).

3.2 Mapping to Dirac fermion in static curved space

We will now relate the TB Hamiltonian to the Dirac Hamiltonian in curved space derived in section 2.2. Since the local velocity \tilde{v}_{ij} is symmetric by construction, we can rename it as follows

$$\tilde{v}_{aj} \rightarrow \tilde{v}_a^j \quad (a = 1, 2; i = 1, 2). \quad (3.6)$$

We can rewrite the tight binding Hamiltonian as ²

$$H^{TB} = v_F \int d^2\mathbf{x} \psi^\dagger \left(-i\tilde{v}_a^i(\mathbf{x})\sigma^a \overleftrightarrow{\partial}_i - \sigma^a A_a^s(\mathbf{x}) \right) \psi. \quad (3.7)$$

Comparing the TB Hamiltonian (3.7) and the Dirac Hamiltonian in static curved space (2.13) we obtain the explicit map

$$e_a^i(\mathbf{x}) = \tilde{v}_{ai}(\mathbf{x}), \quad (3.8)$$

$$A_i(\mathbf{x}) = e_i^a(\mathbf{x})A_a^s(\mathbf{x}), \quad (3.9)$$

$$\tilde{\Psi}(\mathbf{x}) = \psi(\mathbf{x}), \quad (3.10)$$

where $e_i^a(\mathbf{x})$ is the inverse vielbein such that $e_i^a(\mathbf{x})e_b^i(\mathbf{x}) = \delta_b^a$. Note that $\tilde{\Psi}(\mathbf{x})$ and $\psi(\mathbf{x})$ share the same definition of inner product (without $\sqrt{\hat{g}}$). We can confirm that the effective theory of strained graphene can always be mapped to a field theory of a Dirac fermion in static curved space.

From the inverse vielbein $e_i^a(\mathbf{x})$, one can derive the spatial component of the metric $g_{ij}(\mathbf{x}) = e_i^a(\mathbf{x})e_j^a(\mathbf{x})$. The Gaussian curvature in two dimensions can be calculated using the formula [35]

$$\mathcal{K}(\mathbf{x}) = \frac{\mathcal{R}_{1212}(\mathbf{x})}{\hat{g}(\mathbf{x})}, \quad (3.11)$$

where the Riemann curvature tensor is given by

$$\mathcal{R}_{ijkl} = g_{lq} \left(\partial_i \Gamma_{jk}^q - \partial_j \Gamma_{ik}^q + \Gamma_{jk}^p \Gamma_{ip}^q - \Gamma_{ik}^p \Gamma_{jp}^q \right). \quad (3.12)$$

The magnetic field in static curved space is defined as

$$B(\mathbf{x}) = \frac{\partial_1 A_2(\mathbf{x}) - \partial_2 A_1(\mathbf{x})}{\sqrt{\hat{g}(\mathbf{x})}}. \quad (3.13)$$

The energy of Landau levels for constant curvature and magnetic field is [36]

$$E_n(B, \mathcal{K}) = v_F \text{sgn}(n) \sqrt{2|nB| + n^2 \mathcal{K}}, \quad (3.14)$$

which is valid for $\frac{|B|}{\mathcal{K}} > \frac{1}{2}$ if $\mathcal{K} > 0$, and for $\frac{|B|}{|\mathcal{K}|} > (|n| + \frac{1}{2})$ if $\mathcal{K} < 0$.

Note that we use the torsionless spin connection in the definition (2.3) because we only consider the strain without defects (disclinations and dislocations). In general, one needs to map the effective theory of strained TB model with defects to the field theory in curved space with torsion if there are defects in the strained lattice. The field theory in curved space with torsion and the relation to the lattice with defects was studied in [37–39].

²By renaming i to a .

4 Second-order calculation

We strain the lattice such that the positions of the lattice sites are displaced as

$$\mathbf{x} \rightarrow \mathbf{x} + \mathbf{u}(\mathbf{x}). \quad (4.1)$$

Let us propose the following strain profile, which produces a constant magnetic field at first order in the strain

$$\mathbf{u} = \frac{u_B}{L} \begin{pmatrix} 2xy \\ x^2 - y^2 \end{pmatrix} \quad (4.2)$$

where u_B is a dimensionless number and L is the total size of the lattice. For our approximations to hold, we want the change in the distance of neighbouring atoms due to strain to be less than the lattice spacing a . This implies

$$a\nabla\mathbf{u} \ll a \quad (4.3)$$

and if we want this to hold up to the edge of the lattice we therefore require $u_B \ll 1$. The hopping usually depends on the distance between nearest-neighbour atoms as

$$t_n(\mathbf{x}) = t_0 e^{-\beta(|\mathbf{l}_n + \mathbf{u}(\mathbf{x} + \mathbf{l}_n) - \mathbf{u}(\mathbf{x})| - a)/a}, \quad (4.4)$$

where $\beta \approx 3$ for real graphene [40]. For the photonic lattice, this form is also valid and β can be tuned. For the purpose of a cleaner numerical match with the field theory, we will rather use a hopping profile that is exactly linear in the displacement with vanishing higher order terms

$$t_n(\mathbf{x}) = t_0 \left(1 - \frac{\beta}{a^2} (\mathbf{u}(\mathbf{x} + \mathbf{l}_n) - \mathbf{u}(\mathbf{x})) \cdot \mathbf{l}_n \right) \quad (4.5)$$

while still carrying out the rest of the calculation to second order in strain. The expression (4.5) for the tunneling results in cleaner LL compared to using the full exponential profile (4.4). So although this form of the tunneling is not exactly the form that is relevant to experiments, we use it to check that our TB numerics reproduce the field theory predictions. It has already been noted in [41, 42] that this strain profile results in cleaner LL.

The detailed derivation of the space-dependent Fermi velocity $\tilde{v}^{ij}(\mathbf{x})$ and the gauge field $A_a^s(\mathbf{x})$ for the tunneling (4.5) is found in Appendix E: the final expressions are (E.13) and (E.15) respectively. We apply the map (3.8)-(3.10) and then use the formulae for the curvature (3.11) and the magnetic field (3.13) from the previous section. For this strain profile, we find curvature

$$\mathcal{K} = -\frac{4}{a^2} \left(\beta \frac{au_B}{L} \right)^2 \quad (4.6)$$

and magnetic field

$$B = \frac{4}{a^2} \beta \frac{au_B}{L} \quad (4.7)$$

We see that we have both a constant curvature and constant magnetic field, as desired.

We can also perform the same calculation for the exponential tunneling (4.4). We need to expand to second order in the strain, since we want to investigate the effect of curvature on the Landau levels, which appears at that order for the given profile. The calculation is performed in Appendix F. The expressions for the curvature and magnetic field in that case are given by equations (F.21) and (F.22) respectively. We emphasize that our approach can

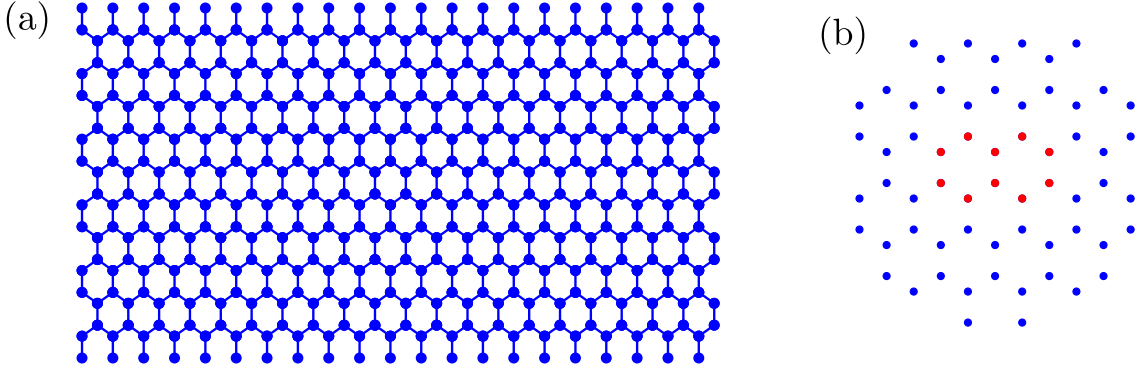


Figure 1: (a) Sketch of the choice of lattice for a smaller total number of atoms, illustrating the choice of the boundary of the region. (b) Sketch of the central region of the lattice with the 10 central sites that are used to calculate the LDOS coloured in red.

be used to compute \mathcal{K} and B to arbitrary order in the strain. Beyond the second order we observe that the curvature and magnetic field are no longer constant in space.

We note that it is possible to have non-zero curvature at first order in the strain if $\nabla \cdot \mathbf{u} \neq 0$, however in this case the distance between neighbouring sites will significantly differ from a far away from the centre of the lattice. In addition this leads to the scalar potential we neglected. For the numerical calculation this results in blurred out LL.

5 Numerical calculation

By exactly diagonalizing the Hamiltonian, we can determine the spectrum and compare to the field theory calculation. We use a lattice with around 10,000 sites and plot the integrated local density of states (LDOS) $D(\varepsilon)$ for 10 sites closest to the centre of the lattice, as shown in Fig. 1. We need to make sure to include the same number of A and B sublattice sites when calculating the LDOS, since for higher LL the wavefunctions have different amplitudes on both sublattices. The LDOS is

$$D(\varepsilon) = \sum_n \Theta(\varepsilon - \varepsilon_n) \sum_{i=1}^{10} |\psi_n(\mathbf{x}_i)|^2 \quad (5.1)$$

where the first sum is over all eigenvalues ε_n with corresponding normalized eigenfunction $\psi_n(\mathbf{x})$ and the second sum is over the 10 central sites at positions \mathbf{x}_i . $\Theta(x)$ denotes the Heaviside step function. We use the strain profile (4.2).

Below, we plot the LDOS and compare to the expression (3.14) with B and \mathcal{K} given by (4.7) and (4.7) respectively. The spectrum shows clear jumps at the energies corresponding to the Landau levels.

We see that we need to include the effect of the non-zero curvature in order to accurately fit the positions of the Landau levels. We note that the zeroth LL is the sharpest, the reason being that the existence of a certain number of zero-energy states is guaranteed by an index theorem, which does not rely on the magnetic field being uniform [43]. Higher LL are smeared

out since the small momentum expansion that we used to derive the field theory is no longer valid [44].

An additional feature of the QHE in constant curvature is that the LL degeneracy now depends on the LL index n due to the Wen-Zee shift [36, 45]. Unfortunately the LDOS is not a good probe for this effect and we do not see this effect in our numerics. The Wen-Zee shift is a global property. One can derive the LL degeneracy using the Index Theorem, which requires an integral over the entire manifold [36]. In addition, the derivation of the Wen-Zee shift uses the assumption that we have a sphere with a constant curvature, which we do not have here. We only have a manifold with approximately constant curvature near the center. So in principle, one should not expect to obtain Wen-Zee shift from LDOS of the current setup.

6 Comparison to previous work

In this section we consider how our results compare with other works that have addressed the same problem. Ref. [1] considered only the linear expansion, and obtained only a part of Eq. (3.3). In Appendix E we explain how their results are reconciled with ours once the next order in the derivatives is included, which is essential to compute curvature and magnetic field to second order in strain.

The same strain profile that we used is also studied in [46]. Their expression for the energy levels differs from our result in two regards. On the one hand they employ a different definition of the emergent magnetic field, namely $\mathbf{H} = \nabla \times \mathbf{A}$, whereas we use the curved space formula $\mathbf{B} = (\nabla \times \mathbf{A})/\sqrt{g}$. This accounts for the apparent difference between our result and that of [46], when written directly in terms of the strain field the results are the same, except that [46] neglects the curvature correction to the energy levels (the n^2 term).

We emphasize again, that in contrast to [6, 46] we perform the rescaling of the field (2.11) in order to obtain the correct inner product (2.12). The important point to realize is that the Hamiltonian (2.9) is Hermitian with respect to the scalar product (2.10), so that the Hamiltonian (2.9) cannot be directly compared to the tight binding Hamiltonian of strained graphene. The field redefinition (2.11) is an essential step to map the effective theory of strained graphene to the theory of a Dirac fermion in curved space. The formalism is backed up by our numerical results, where we have a perfect matching with a highly non-trivial analytical form of the Landau level energy. Our field redefinition (2.11) and the maps in Sec. 3.2 are our new contributions to the literature.

7 Conclusions

We have shown that the effective low-energy theory governing strained graphene is a Dirac fermion in curved space coupled to an artificial gauge field. In the case where the strain profile is engineered such to give a constant magnetic field and constant curvature, we obtain the well-known Landau levels for a relativistic fermion, with a modification due to the curvature. These corrections are seen in exact diagonalization of the Hamiltonian and the agreement between the theory and the numerics vindicates our low-energy theory. This is the first term that these corrections to the Landau levels due to curvature have been seen in strained

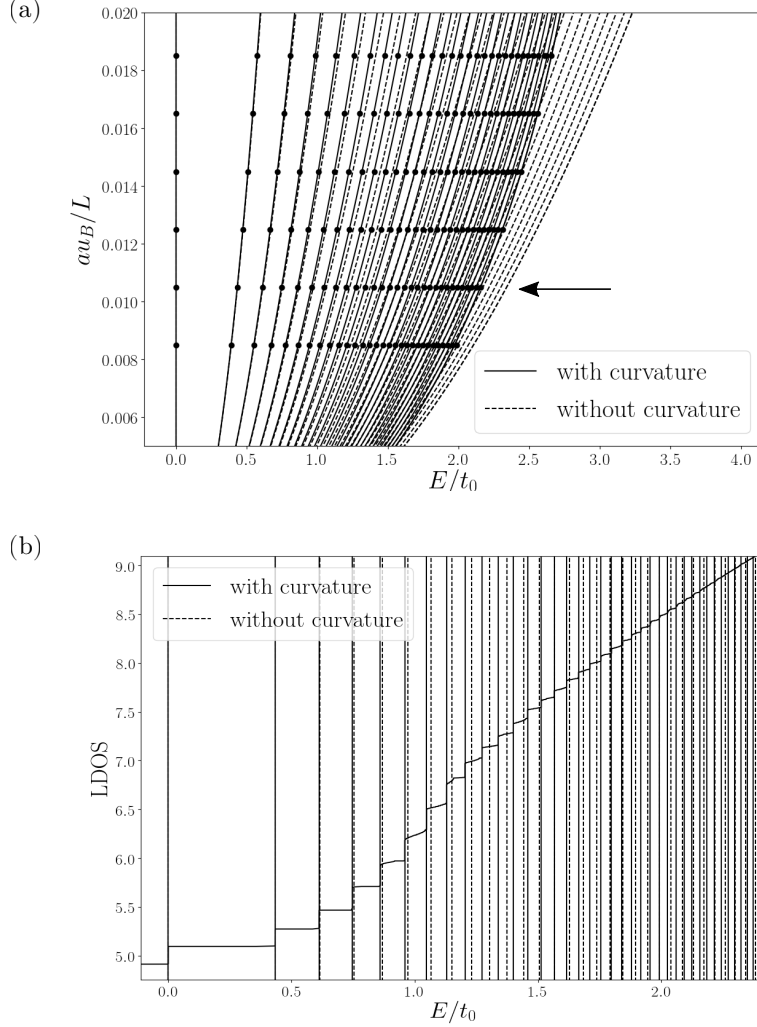


Figure 2: Tight-binding results for the strain profile (4.2) with TB parameter $\beta = 1$. We perform exact diagonalization (ED) of a lattice with 10,000 sites. (a) The circles show the location of the Landau levels as determined by the peaks in the local density of states (LDOS) as a function of the applied strain au_B/L . We compare the prediction (3.14) with (solid curve) and without curvature (dashed curve) to the data and see that only the model with curvature accurately fits the data. (b) Integrated LDOS for the parameter $au_B/L = 0.0105$, which is indicated by the arrow in figure (a). We plot the expected position of the energy levels with and without the additional contribution from the curvature. Again, it can clearly be seen that the curvature term is important in order to match the field theory result to the ED result.

graphene.

In the derivation, the factors of $\hat{g}^{1/4}$ and $\sqrt{\hat{g}}$ in (2.11) and (3.13) respectively are subtle points that were missed in previous works on this topic. We also emphasize that we have settled the point about whether to expand about the shifted or unshifted \mathbf{K} -points. The numerical results support our analytical formalism.

Besides straining ordinary graphene, there are two other promising platforms that offer more control over the desired strain profile. The first is a photonic lattice, where waveguides are etched into a crystal in a hexagonal arrangement and hopping of photons between waveguides is well-described by a tight-binding model. Signatures of the quantum Hall effect in the photonic analogue of strained graphene have already been observed [47–50]. The main signature seen so far in the photonic analogue are the robust chiral edge modes. It would be interesting to extend this work in order to be able to measure the Landau levels themselves. However, this would require measuring the local density of states, something that has proved elusive in this system so far. On the other hand, a system which offers a way of measuring energies directly is the sonic lattice [51–53]. A similar Hamiltonian has also been constructed for ultracold atoms in an optical lattice [54].

An avenue for further research is considering different strain profiles that may be able to simulate more exotic gravitational analogues. For example, it has been proposed to construct a graphene analogue of a wormhole [55].

Acknowledgements

F.J. especially thanks Joel E. Moore for insightful discussions on this topic. D.X.N would like to thank Paul Wiegmann and Dam Thanh Son for a discussion on the UV completeness of the effective theory. The authors also thank Carlos Hoyos, Steve Simon and Christopher Herzog for comments on a previous version of this manuscript. The calculation of the curvature from the metric was performed using the Mathematica package ‘Riemannian Geometry and Tensor Calculus’ (RGTC) [56]. This work was supported by grants EP/N01930X/1 and EP/S020527/1. DXN was supported partially by Brown Theoretical Physics Center.

A 2 + 1D Dirac fermion in static curved space

A.1 Action in curved space-time

We recall the action (2.7) of a spin- $\frac{1}{2}$ Dirac fermion in curved space-time

$$\mathcal{S} = i \int d^3x \sqrt{|g|} \bar{\Psi} \gamma^\mu (\partial_\mu - iA_\mu - \frac{i}{2} \omega_\mu^{\alpha\beta} \sigma_{\alpha\beta}) \Psi. \quad (\text{A.1})$$

The Hermitian conjugate of (A.1) is

$$\mathcal{S}^\dagger = i \int d^3x \sqrt{|g|} e_\alpha^\mu [-\partial_\mu \Psi^\dagger (\gamma^\alpha)^\dagger - i \Psi^\dagger A_\mu (\gamma^\alpha)^\dagger - \frac{i}{2} \Psi^\dagger \omega_\mu^{\beta\gamma} (\sigma_{\beta\gamma})^\dagger (\gamma^\alpha)^\dagger] (\gamma^0)^\dagger \Psi. \quad (\text{A.2})$$

We then use the following identities

$$(\gamma^0)^\dagger = \gamma^0, \quad (\gamma^\alpha)^\dagger \gamma^0 = \gamma^0 \gamma^\alpha \quad (\text{A.3})$$

together with the definition of $\sigma_{\alpha\beta}$ and rewrite the action \mathcal{S}^\dagger as

$$\mathcal{S}^\dagger = i \int d^3x \sqrt{|g|} \bar{\Psi} \left[\gamma^\mu (-\overleftarrow{\partial}_\mu - iA_\mu) - \frac{i}{2} \omega_\mu^{\alpha\beta} \sigma_{\alpha\beta} \gamma^\mu \right] \Psi, \quad (\text{A.4})$$

where $\overleftarrow{\partial}_\mu$ only acts on $\bar{\Psi}$ respectively. We now will show that the actions (A.1) and (2.8) are equivalent up to a surface term. Define $\mathcal{S}' = \frac{1}{2}(\mathcal{S} + \mathcal{S}^\dagger)$. Then from (A.1) and (A.4), we have

$$\mathcal{S} - \mathcal{S}' = \frac{i}{2} \int d^3x \sqrt{|g|} \bar{\Psi} \left(\gamma^\mu \overrightarrow{\nabla}_\mu + \overleftarrow{\nabla}_\mu \gamma^\mu \right) \Psi, \quad (\text{A.5})$$

where the covariant derivatives $\overrightarrow{\nabla}_\mu, \overleftarrow{\nabla}_\mu$, which are defined as

$$\overrightarrow{\nabla}_\mu = \overrightarrow{\partial}_\mu - \frac{i}{2} \omega_\mu^{\alpha\beta} \sigma_{\alpha\beta}, \quad \overleftarrow{\nabla}_\mu = \overleftarrow{\partial}_\mu + \frac{i}{2} \omega_\mu^{\alpha\beta} \sigma_{\alpha\beta}, \quad (\text{A.6})$$

only act on Ψ and $\bar{\Psi}$. We use the expression of the covariant derivative of the gamma matrices [57]

$$\nabla_\mu \gamma_\nu = \partial_\mu \gamma_\nu - \frac{i}{4} \omega_\mu^{\alpha\beta} [\sigma_{\alpha\beta}, \gamma_\nu] - \Gamma_{\mu\nu}^\rho \gamma_\rho, \quad (\text{A.7})$$

which implies that γ_μ is not only a covariant vector with index μ but also has two spinor indices which need to be taken care of properly in the definition of the covariant derivative. Using the anti-commutation relation of gamma matrices and the definition (2.6), we have

$$\nabla_\mu \gamma_\nu = \gamma^\alpha \left(\partial_\mu e_{\alpha\nu} + \omega_{\mu\alpha\beta} e_\nu^\beta - \Gamma_{\mu\nu}^\rho e_{\alpha\rho} \right). \quad (\text{A.8})$$

The right hand side of the above equation vanishes due to the tetrad postulate (2.4), we then can rewrite equation (A.5) as

$$\mathcal{S} - \mathcal{S}' = \frac{i}{2} \int d^3x \sqrt{|g|} \nabla_\mu (\bar{\Psi} \gamma^\mu \Psi) \quad (\text{A.9})$$

$$= \frac{i}{2} \int d^3x \sqrt{|g|} \left[\partial_\mu (\bar{\Psi} \gamma^\mu \Psi) + \Gamma_{\mu\nu}^\mu (\bar{\Psi} \gamma^\nu \Psi) \right], \quad (\text{A.10})$$

where we recognize that the right hand side is the covariant derivative of the current density operator. We then use the identity $\Gamma_{\mu\nu}^\mu = \frac{\partial \ln(|g|)}{\partial x^\nu}$ to show that the above equation is just a surface term

$$\mathcal{S} - \mathcal{S}' = \frac{i}{2} \int d^3x \partial_\mu \left(\sqrt{|g|} \bar{\Psi} \gamma^\mu \Psi \right). \quad (\text{A.11})$$

So indeed we confirmed that \mathcal{S} and \mathcal{S}' are equivalent up to a surface term and we can use either of them for the theory of a $2 + 1D$ Dirac fermion in curved space-time.

A.2 Hamiltonian in static curved space

Combining equations (A.1) and (A.4), we obtain

$$\mathcal{S}' = i \int d^3x \sqrt{|g|} \bar{\Psi} \left[\gamma^\mu (\overrightarrow{\partial}_\mu - iA_\mu) + \frac{i}{4} \omega_\mu^{\alpha\beta} \{ \sigma_{\alpha\beta}, \gamma^\mu \} e_\rho^\mu \right] \Psi, \quad (\text{A.12})$$

where $\overleftrightarrow{\partial}_\mu = \frac{1}{2}(\overrightarrow{\partial}_\mu - \overleftarrow{\partial}_\mu)$ only acts on fermion fields. From the definition of the static curved space vielbein, we see that the anti-commutator in the above equation vanishes. Then in static curved space, we obtain the action

$$\mathcal{S}' = i \int d^3x \sqrt{\hat{g}} \bar{\Psi} \left[\gamma^\mu (\overleftrightarrow{\partial}_\mu - iA_\mu) \right] \Psi, \quad (\text{A.13})$$

with corresponding Hermitian Hamiltonian

$$H = -i \int d^2x \sqrt{\hat{g}} \left[\Psi^\dagger e_a^i \sigma^a (\overleftrightarrow{\partial}_i - iA_i) \Psi - iA_0 \Psi^\dagger \Psi \right], \quad (\text{A.14})$$

where $\hat{g} = \det(g_{ij})$. If we consider the Dirac action with the Fermi velocity v_F replacing the speed of light,

$$\mathcal{S} = i \int d^3x \sqrt{|g|} \bar{\Psi} \left[\gamma^0 (\overrightarrow{\nabla}_0 - iA_0) + v_F \gamma^i (\overrightarrow{\nabla}_i - iA_i) \right] \Psi, \quad (\text{A.15})$$

one can repeat the calculation in the previous section with slight modifications and obtain the Hermitian Hamiltonian in static curved space

$$H = -i \int d^2x \sqrt{\hat{g}} \left[\Psi^\dagger v_F e_a^i \sigma^a (\overleftrightarrow{\partial}_i - iA_i) \Psi - iA_0 \Psi^\dagger \Psi \right], \quad (\text{A.16})$$

If we consider an applied magnetic field only and chose the Coulomb gauge $A_0 = 0$, the Hamiltonian has the form

$$H = -iv_F \int d^2x \sqrt{\hat{g}} \Psi^\dagger e_a^i \sigma^a (\overleftrightarrow{\partial}_i - iA_i) \Psi. \quad (\text{A.17})$$

The above equation is nothing but the Hamiltonian (2.9) in the main text.

Now we showed in (A.11) that \mathcal{S} and \mathcal{S}' differ by a total derivative, hence they should give rise to the same equation of motion for the field Ψ . How does this reconcile with the fact that the action \mathcal{S} in (A.1) has a spin connection term while the action \mathcal{S}' (valid for static curved space) in (A.13) does not? When we compute the equation of motion for Ψ from (A.13), we need to integrate by parts to convert the derivative $\overleftrightarrow{\partial}_\mu$ into a derivative ∂_μ acting only on the right. In this process, we end up with a derivative of $\sqrt{\hat{g}}$ and a derivative of the vielbein (since the vielbein is implicit in γ^μ). The term including the derivative of $\sqrt{\hat{g}}$ is cancelled after we redefine the Dirac field as in equation (2.11). The derivative of the spin connection term can be shown to be precisely equivalent to the term coming from the spin connection when the equation of motion is derived from (A.1)³.

B Derivation of effective tight-binding Hamiltonian

The TB Hamiltonian (3.1) is Hermitian by construction. We will map the final result to the Hamiltonian of a $2 + 1D$ Dirac fermion in static curved space. Since the Hamiltonian is

³We note that in [1], there is a term with the derivative the space-dependent Fermi velocity in the equation of motion, which corresponds to the derivative of the vielbein after the mapping we will introduce in section 3.2.

Hermitian, the corresponding action is \mathcal{S}' instead of \mathcal{S} , and one then discover that the mapped Hamiltonian doesn't have the spin-connection term which is (2.13). In the continuum limit, we define the field operator of sub-lattice A and B as well as their Fourier modes:

$$\psi_I(\mathbf{x}) = \sum_{\mathbf{k}} \frac{1}{N} e^{-i\mathbf{k}\mathbf{x}} \psi_I(\mathbf{k}), \quad \psi_I(\mathbf{k}) = \sum_{\mathbf{x}} e^{i\mathbf{k}\mathbf{x}} \psi_I(\mathbf{x}). \quad (\text{B.1})$$

where $I = A, B$ with the normalization

$$\sum_{\mathbf{x}} e^{i\mathbf{k}\mathbf{x}} = N\delta_{\mathbf{k},0}, \quad \sum_{\mathbf{k}} e^{i\mathbf{k}\mathbf{x}} = N\delta_{\mathbf{x},0}, \quad (\text{B.2})$$

We can rewrite the Hamiltonian (3.1) as

$$H^{TB} = \sum_{n, \mathbf{R}_i} \sum_{\mathbf{k}, \mathbf{k}'} \frac{1}{N^2} t_n(\mathbf{R}_i) \left(\psi_A^\dagger(\mathbf{k}) \psi_B(\mathbf{k}') e^{i\mathbf{k}\mathbf{R}_i - i\mathbf{k}'(\mathbf{R}_i + \mathbf{l}_n)} + \psi_B^\dagger(\mathbf{k}') \psi_A(\mathbf{k}) e^{-i\mathbf{k}\mathbf{R}_i + i\mathbf{k}'(\mathbf{R}_i + \mathbf{l}_n)} \right) \quad (\text{B.3})$$

we redefine $\mathbf{k} \leftrightarrow \mathbf{k}'$ on the second term and define

$$\psi(\mathbf{k}) = \begin{pmatrix} \psi_A(\mathbf{k}) \\ \psi_B(\mathbf{k}) \end{pmatrix} \quad (\text{B.4})$$

to obtain the matrix form equation

$$H^{TB} = \sum_{n, \mathbf{k}, \mathbf{k}'} \frac{1}{N^2} t_n(\mathbf{k} - \mathbf{k}') \psi^\dagger(\mathbf{k}) \begin{pmatrix} 0 & e^{-i\mathbf{k}'\mathbf{l}_n} \\ e^{i\mathbf{k}\mathbf{l}_n} & 0 \end{pmatrix} \psi(\mathbf{k}'), \quad (\text{B.5})$$

with the definition of Fourier transformation

$$t_n(\mathbf{x}) = \sum_{\mathbf{k}} \frac{1}{N} e^{-i\mathbf{k}\mathbf{x}} t_n(\mathbf{k}), \quad t_n(\mathbf{k}) = \sum_{\mathbf{x}} e^{i\mathbf{k}\mathbf{x}} t_n(\mathbf{x}). \quad (\text{B.6})$$

B.1 Expansion around the \mathbf{K} point

We define the two Dirac points $\mathbf{K} = (\frac{4\pi}{3\sqrt{3}a}, 0)$ and $\mathbf{K}' = -\mathbf{K}$. We then define $\mathbf{k} = \mathbf{q} + \mathbf{K}$, and redefine $\psi(\mathbf{K} + \mathbf{q}) \rightarrow \psi(\mathbf{q})$. Expanding up to second order in the small momenta \mathbf{q} and \mathbf{q}' , we find

$$H^{TB} = i \sum_{n, \mathbf{q}, \mathbf{q}'} \frac{1}{N^2} t_n(\mathbf{q} - \mathbf{q}') \psi^\dagger(\mathbf{q}) \frac{\sigma \cdot \mathbf{l}_n}{a} \sigma^3 \times \begin{pmatrix} 1 + iq_i l_n^i - \frac{1}{2} q_i q_j l_n^i l_n^j & 0 \\ 0 & 1 - iq'_i l_n^i - \frac{1}{2} q'_i q'_j l_n^i l_n^j \end{pmatrix} \psi(\mathbf{q}') \quad (\text{B.7})$$

we then define

$$\mathbf{Q} = \frac{1}{2}(\mathbf{q} + \mathbf{q}'), \quad \mathbf{s} = \frac{1}{2}(\mathbf{q} - \mathbf{q}'). \quad (\text{B.8})$$

We can rewrite the above Hamiltonian in the following form

$$H^{TB} = i \sum_{n, \mathbf{Q}, \mathbf{s}} \frac{1}{4N^2} t_n(2\mathbf{s}) \psi^\dagger(\mathbf{Q} + \mathbf{s}) \frac{\sigma \cdot \mathbf{l}_n}{a} \sigma^3 \times \begin{pmatrix} 1 + i(Q_i + s_i) l_n^i - \frac{1}{2} (Q_i + s_i)(Q_j + s_j) l_n^i l_n^j & 0 \\ 0 & 1 - i(Q_i - s_i) l_n^i - \frac{1}{2} (Q_i - s_i)(Q_j - s_j) l_n^i l_n^j \end{pmatrix} \psi(\mathbf{Q} - \mathbf{s}), \quad (\text{B.9})$$

where the factor $1/4$ comes from the change of variable (Jacobian). Using the Fourier transformation to convert it back to the coordinate space, we obtain

$$H^{TB} = i \sum_{n, \mathbf{Q}, \mathbf{s}, \mathbf{x}, \mathbf{y}} \frac{1}{4N^2} t_n(2\mathbf{s}) e^{-i\mathbf{Q}(\mathbf{x}-\mathbf{y}) - i\mathbf{s}(\mathbf{x}+\mathbf{y})} \times \\ \psi^\dagger(\mathbf{x}) \frac{\sigma \cdot \mathbf{l}_n}{a} \sigma^3 \left(1 + i(Q_i + s_i) l_n^i - \frac{1}{2}(Q_i + s_i)(Q_j + s_j) l_n^i l_n^j \right. \\ \left. 1 - i(Q_i - s_i) l_n^i - \frac{1}{2}(Q_i - s_i)(Q_j - s_j) l_n^i l_n^j \right) \psi(\mathbf{y}). \quad (\text{B.10})$$

Using the identity $\sum_{\mathbf{Q}} e^{-i\mathbf{Q}(\mathbf{x}-\mathbf{y})} = 4N\delta_{\mathbf{x}-\mathbf{y},0}$, and the identities

$$\sum_{\mathbf{x}, \mathbf{y}} iQ_i e^{-i\mathbf{Q}(\mathbf{x}-\mathbf{y}) - i\mathbf{s}(\mathbf{x}+\mathbf{y})} \psi^\dagger(\mathbf{x}) \Sigma \psi(\mathbf{y}) = \sum_{\mathbf{x}, \mathbf{y}} e^{-i\mathbf{Q}(\mathbf{x}-\mathbf{y}) - i\mathbf{s}(\mathbf{x}+\mathbf{y})} \frac{1}{2} \left(\frac{\partial \psi^\dagger(\mathbf{x})}{\partial x^i} \Sigma \psi(\mathbf{y}) - \psi^\dagger(\mathbf{x}) \Sigma \frac{\partial \psi(\mathbf{y})}{\partial y^i} \right), \quad (\text{B.11})$$

$$\sum_{\mathbf{x}, \mathbf{y}} i s_i e^{-i\mathbf{Q}(\mathbf{x}-\mathbf{y}) - i\mathbf{s}(\mathbf{x}+\mathbf{y})} \psi^\dagger(\mathbf{x}) \Sigma \psi(\mathbf{y}) = \sum_{\mathbf{x}, \mathbf{y}} e^{-i\mathbf{Q}(\mathbf{x}-\mathbf{y}) - i\mathbf{s}(\mathbf{x}+\mathbf{y})} \frac{1}{2} \left(\frac{\partial \psi^\dagger(\mathbf{x})}{\partial x^i} \Sigma \psi(\mathbf{y}) + \psi^\dagger(\mathbf{x}) \Sigma \frac{\partial \psi(\mathbf{y})}{\partial y^i} \right) \quad (\text{B.12})$$

up to surface terms, where Σ is any 2×2 matrix, we go back to position space, the results (3.2) together with (3.3) and (3.4) follow after we replace

$$\sum_{\mathbf{x}} \rightarrow \frac{1}{a^2} \int d^2\mathbf{x} \quad (\text{B.13})$$

and integrate by parts. We discard all terms that have more than one derivative acting on fermion fields, since these cannot be brought into the form of the Dirac Hamiltonian. We also discard terms that have more than one derivative acting on the hopping $t_n(\mathbf{x})$ and terms with higher order in $\overleftrightarrow{\partial}$. There terms are all higher-order in the momentum and will be relevant far from the Dirac points, ie once we get to high Landau levels.

B.2 Expansion around the \mathbf{K}' point

Repeating the same calculations in the above subsection, we obtain the effective Hamiltonian

$$H^{TB} = \int d^2\mathbf{x} v_F \psi^\dagger(\mathbf{x}) \left(i\sigma_i \tilde{v}^{ij}(\mathbf{x}) \overleftrightarrow{\partial}_j - \sigma^i A_i^s(\mathbf{x}) \right) \psi'(\mathbf{x}) \quad (\text{B.14})$$

where $\tilde{v}^{ij}(\mathbf{x})$ and $A_i(\mathbf{x})$ are the same as in (3.3) and (3.4). The definition of $\psi'(\mathbf{x})$ is

$$\psi'(\mathbf{x}) = e^{-i\mathbf{K}\mathbf{x}} \begin{pmatrix} \psi_B(\mathbf{x}) \\ \psi_A(\mathbf{x}) \end{pmatrix} \quad (\text{B.15})$$

Notice again the minus sign in the derivative term of (B.14) in comparison with (3.2).

B.3 Valley dual transformation

From (3.2) and (B.14) we derive the Schrödinger equation of the effective theory near \mathbf{K}

$$-v_F \sigma_i \left(i\tilde{v}^{ij}(\mathbf{x}) \partial_j + \frac{i}{2} \partial_j \tilde{v}^{ij}(\mathbf{x}) + A_i^s(\mathbf{x}) \right) \psi(\mathbf{x}) = E \psi(\mathbf{x}), \quad (\text{B.16})$$

and near the \mathbf{K}' point

$$v_F \sigma_i \left(i\tilde{v}^{ij}(\mathbf{x}) \partial_j + \frac{i}{2} \partial_j \tilde{v}^{ij}(\mathbf{x}) - A_i^s(\mathbf{x}) \right) \psi'(\mathbf{x}) = E \psi'(\mathbf{x}). \quad (\text{B.17})$$

We take the complex conjugate of equation (B.17) then multiply by σ^1 and use the identity

$$\sigma^1(\sigma_i)^* = \sigma_i\sigma^1 \quad (i = 1, 2), \quad (\text{B.18})$$

to obtain

$$-v_F\sigma_i \left(i\tilde{v}^{ij}(\mathbf{x})\partial_j + \frac{i}{2}\partial_j\tilde{v}^{ij}(\mathbf{x}) + A_i^s(\mathbf{x}) \right) \sigma^1\psi'^*(\mathbf{x}) = E\sigma^1\psi'^*(\mathbf{x}), \quad (\text{B.19})$$

which is the same as the Schrödinger equation of the effective theory near the \mathbf{K} point (B.16). From the above transformation, we see that each eigenenergy of the effective Hamiltonian near \mathbf{K}' corresponds to the same eigenenergy of the effective Hamiltonian near \mathbf{K} . We also see that the transformation of the wave-function has the form of a valley dual (VD) transformation in $2 + 1D$ ⁴

$$\psi'(x) \xrightarrow{VD} \sigma^1\psi'^*(\mathbf{x}). \quad (\text{B.20})$$

Using equation (B.15), we see that under the P-H transformation, we obtain

$$\psi'(x) \xrightarrow{VD} e^{i\mathbf{K}\mathbf{x}} \begin{pmatrix} \psi_A^*(\mathbf{x}) \\ \psi_B^*(\mathbf{x}) \end{pmatrix}. \quad (\text{B.21})$$

The VD transformations transform the effective theory near \mathbf{K} into the effective field theory near \mathbf{K}' .

C Which \mathbf{K} point should one expand about?

In this appendix, we analyze the expanding around space-dependent \mathbf{K} point approach in Ref [4]. We will show that by careful calculation, this approach is ill-defined at the higher order in strain field. The starting point is—as before—(B.5)

$$H^{TB} = \sum_{n,\mathbf{k},\mathbf{k}'} \frac{1}{N^2} t_n(\mathbf{k} - \mathbf{k}') \psi^\dagger(\mathbf{k}) \begin{pmatrix} 0 & e^{-i\mathbf{k}'\mathbf{l}_n} \\ e^{i\mathbf{k}\mathbf{l}_n} & 0 \end{pmatrix} \psi(\mathbf{k}'), \quad (\text{C.1})$$

and we define the new variables

$$\mathbf{Q} = \frac{1}{2}(\mathbf{k} + \mathbf{k}'), \quad \mathbf{s} = \frac{1}{2}(\mathbf{k} - \mathbf{k}'). \quad (\text{C.2})$$

Beware that this definition is not the same as (B.8) due to the difference between \mathbf{k} and \mathbf{q} . Remembering the Jacobian for this transformation, we obtain

$$H^{TB} = \sum_{n,\mathbf{s},\mathbf{Q}} \frac{1}{4N^2} t_n(2\mathbf{s}) \psi^\dagger(\mathbf{Q} + \mathbf{s}) \begin{pmatrix} 0 & e^{-i(\mathbf{Q}-\mathbf{s})\mathbf{l}_n} \\ e^{i(\mathbf{Q}+\mathbf{s})\mathbf{l}_n} & 0 \end{pmatrix} \psi(\mathbf{Q} - \mathbf{s}), \quad (\text{C.3})$$

Now define

$$H^{TB} = \sum_{\mathbf{s},\mathbf{Q}} \frac{1}{4N^2} \psi^\dagger(\mathbf{Q} + \mathbf{s}) \hat{H}^{TB}(\mathbf{Q}, \mathbf{s}) \psi(\mathbf{Q} - \mathbf{s}), \quad (\text{C.4})$$

where

$$\hat{H}^{TB}(\mathbf{Q}, \mathbf{s}) = \sum_n t_n(2\mathbf{s}) \begin{pmatrix} 0 & e^{-i(\mathbf{Q}-\mathbf{s})\mathbf{l}_n} \\ e^{i(\mathbf{Q}+\mathbf{s})\mathbf{l}_n} & 0 \end{pmatrix} \quad (\text{C.5})$$

We now follow Ref [4] and define the spatially-dependent \mathbf{K} -point via

$$\sum_n t_n(2\mathbf{s}) \begin{pmatrix} 0 & e^{-i\mathbf{K}^\pm(2\mathbf{s})\mathbf{l}_n} \\ e^{i\mathbf{K}^\pm(2\mathbf{s})\mathbf{l}_n} & 0 \end{pmatrix} = 0 \quad (\text{C.6})$$

⁴It looks similar to the particle-hole (PH) transformation in [58]. However, in our case, we only have the transformation of the wave-function instead of the field operator as in [58]. As a consequence, a particle field near \mathbf{K} maps to a particle field near \mathbf{K}' .

We then expand $\hat{H}^{TB}(\mathbf{Q}, \mathbf{s})$ around $(\mathbf{K}^\pm, \mathbf{0})$.

$$\hat{H}^{TB}(\mathbf{Q}, \mathbf{s}) = i\sigma^3[(\mp\sigma^2\mathbf{f}_2(2\mathbf{s}) + \sigma^1\mathbf{f}_1(2\mathbf{s}))(\mathbf{Q} - K^\pm(2\mathbf{s})) - (\sigma^1\mathbf{f}_1(2\mathbf{s}) \mp \sigma^2\mathbf{f}_2(2\mathbf{s}))\sigma^3\mathbf{s}] \quad (\text{C.7})$$

where the expressions for $\mathbf{f}_{1,2}(2\mathbf{s})$ and $K^\pm(2\mathbf{s})$ can be found in [4]. Let us write $\mathbf{K}^\pm(2\mathbf{s}) = \mathbf{K}^\pm(0) + \delta\mathbf{K}^\pm(2\mathbf{s})$ and consider the term at second order in strain

$$-i\sigma^3\sigma^1\mathbf{f}_1(2\mathbf{s})\delta\mathbf{K}^\pm(2\mathbf{s}) \in \hat{H}^{TB}(\mathbf{Q}, \mathbf{s}) \quad (\text{C.8})$$

Now plugging back into (C.4), we need to evaluate a term of the form

$$\sum_{\mathbf{s}, \mathbf{Q}} \psi^\dagger(\mathbf{Q} + \mathbf{s})\mathbf{f}_1(2\mathbf{s})\delta\mathbf{K}^\pm(2\mathbf{s})\psi(\mathbf{Q} - \mathbf{s}) \quad (\text{C.9})$$

Now we transform back to real space

$$\sum_{\mathbf{x}, \mathbf{y}} \sum_{\mathbf{s}, \mathbf{Q}} \psi^\dagger(\mathbf{x})e^{-i(\mathbf{Q}+\mathbf{s})\cdot\mathbf{x}}\mathbf{f}_1(2\mathbf{s})\delta\mathbf{K}^\pm(2\mathbf{s})\psi(\mathbf{y})e^{i(\mathbf{Q}-\mathbf{s})\cdot\mathbf{y}} \quad (\text{C.10})$$

an evaluating the sum over \mathbf{Q} this becomes

$$N \sum_{\mathbf{x}} \sum_{\mathbf{s}} \psi^\dagger(\mathbf{x})e^{-2i\mathbf{s}\cdot\mathbf{x}}\mathbf{f}_1(2\mathbf{s})\delta\mathbf{K}^\pm(2\mathbf{s})\psi(\mathbf{x}) \quad (\text{C.11})$$

In particular let us study the matrix

$$\sum_{\mathbf{s}} e^{-2i\mathbf{s}\cdot\mathbf{x}}\mathbf{f}_1(2\mathbf{s})\delta\mathbf{K}^\pm(2\mathbf{s}) = \sum_{\mathbf{s}, \mathbf{y}, \mathbf{y}'} e^{-2i\mathbf{s}\cdot\mathbf{x}}e^{2i\mathbf{y}\cdot\mathbf{s}+2i\mathbf{y}'\cdot\mathbf{s}}\mathbf{f}_1(\mathbf{y})\delta\mathbf{K}^\pm(\mathbf{y}') = \frac{N}{2} \sum_{\mathbf{y}} \mathbf{f}_1(\mathbf{y})\delta\mathbf{K}^\pm(\mathbf{x} - \mathbf{y}) \quad (\text{C.12})$$

Now assuming $t_n(\mathbf{x})$ is well-defined, then so will $\mathbf{f}_1(\mathbf{x})$ and $\delta\mathbf{K}^\pm(\mathbf{x})$ be well-defined. However, in general, the sum in (C.12) will not converge. This shows that the expansion about the spatially-dependent \mathbf{K} -point is not well-defined. One can check that it is the case for our choice of strain profile (4.2).

D Uniform dilatation

Let us consider the case of a uniform dilatation of our atomic lattice

$$\mathbf{x}' = \mathbf{x} + \mathbf{u}(\mathbf{x}) = \mathbf{x} + \varepsilon\mathbf{x} \quad (\text{D.1})$$

and so with the hopping (4.5) we find

$$t' = t_0(1 - \beta\varepsilon) \quad (\text{D.2})$$

and hence via (3.3) we have

$$v'_F = (1 - \beta\varepsilon)v_F. \quad (\text{D.3})$$

But now we need to remember that our Dirac Hamiltonian is written in the atomic frame (\mathbf{x} coordinates), instead of in the lab frame (\mathbf{x}' coordinates). If we start with the Hamiltonian in the atomic frame

$$H_{\text{atomic}} = -iv'_F \int d^2\mathbf{x} \psi^\dagger \sigma^i \frac{\partial}{\partial x_i} \psi \quad (\text{D.4})$$

then in the lab frame we obtain, then by virtue of the transformation (D.1) (see e. g. [59] for details)

$$H_{\text{lab}} = \int d^2\mathbf{x}' \psi^\dagger \left[-iv'_F \left(\sigma^i + \frac{\partial u_i}{\partial x'_j} \sigma^j \right) \frac{\partial}{\partial x'_i} + v'_F (\mathbf{K} \cdot \partial'_i \mathbf{u}) \sigma^i \right] \psi \quad (\text{D.5})$$

which simplifies to

$$H_{\text{lab}} = v_F \sigma^i \int d^2 \mathbf{x}' \psi^\dagger \left[-i(1 + \varepsilon - \beta\varepsilon) \frac{\partial}{\partial x'_i} + \varepsilon(1 - \beta\varepsilon) K_i \right] \psi \quad (\text{D.6})$$

Now going to momentum space

$$H_{\text{lab}} = v_F \sigma^i \frac{1}{N^2} \sum_{\mathbf{k}} \psi^\dagger(\mathbf{k}) \left[(1 + \varepsilon - \beta\varepsilon) (k_i - K_i) + \varepsilon(1 - \beta\varepsilon) K_i \right] \psi(\mathbf{k}) \quad (\text{D.7})$$

and up to second order in ε

$$H_{\text{lab}} = \frac{v_F \sigma^i}{N^2} \sum_{\mathbf{k}} \psi^\dagger(\mathbf{k}) \left[(1 + \varepsilon - \beta\varepsilon) (k_i - K_i - \delta K_i) \right] \psi(\mathbf{k}) \quad (\text{D.8})$$

where $\delta K_i = -\varepsilon K_i$. So the final result is consistent with our expectations: We have $a \rightarrow (1 + \varepsilon)a$ and $t \rightarrow t(1 - \beta\varepsilon)$ so $v_F = \frac{3}{2}ta \rightarrow v_F(1 + \varepsilon - \beta\varepsilon)$ and $K = \frac{4\pi}{3\sqrt{3}a} \rightarrow K(1 - \varepsilon)$.

E Second-order calculation: linear tunneling

The hopping has the form

$$t_n(\mathbf{x}) = t_0 \left[1 - \frac{\beta}{a^2} \left(\mathbf{u}(\mathbf{x} + \mathbf{l}_n) - \mathbf{u}(\mathbf{x}) \right) \cdot \mathbf{l}_n \right] \quad (\text{E.1})$$

and

$$\mathbf{u}(\mathbf{x} + \mathbf{l}_n) - \mathbf{u}(\mathbf{x}) \approx (\mathbf{l}_n \cdot \nabla) \mathbf{u} + \frac{1}{2} (\mathbf{l}_n \cdot \nabla)^2 \mathbf{u}. \quad (\text{E.2})$$

The last term in (E.2) is the trigonal warping term. This trigonal warping terms needs to be included when we compute the Christoffel symbols (as well as spin connection) and the curvature, since we work to second order in the derivatives of the strain field $u_i(\mathbf{x})$. This subtlety was missed in the previous work [1]. We then have

$$\frac{1}{a^2} \left(\mathbf{u}(\mathbf{x} + \mathbf{l}_n) - \mathbf{u}(\mathbf{x}) \right) \cdot \mathbf{l}_n \approx \frac{l_n^i l_n^j u_{ij}}{a^2} + \frac{l_n^i l_n^j l_n^k \partial_i u_{jk}}{2a^2} \quad (\text{E.3})$$

where we have defined

$$u_{ij} \equiv \partial_i u_j \quad (\text{E.4})$$

It will be useful to define the following matrices

$$\frac{1}{a} \sum_{n=1}^3 l_n^i = 0, \quad (\text{E.5})$$

$$\frac{1}{a^2} \sum_{n=1}^3 l_n^i l_n^j = \frac{3}{2} \delta^{ij}, \quad (\text{E.6})$$

$$\frac{1}{a^3} \sum_{n=1}^3 l_n^i l_n^j l_n^k = -\frac{3}{4} K^{ijk}, \quad (\text{E.7})$$

$$\frac{1}{a^4} \sum_{n=1}^3 l_n^i l_n^j l_n^k l_n^l = \frac{3}{8} L^{ijkl}, \quad (\text{E.8})$$

The matrices K and L are completely symmetric in all their indices and hence have 4 and 5 independent components respectively. All the entries of these matrices are integers. The independent entries are

$$K^{111} = 0, K^{112} = -1, K^{122} = 0, K^{222} = 1 \quad (\text{E.9})$$

and

$$\begin{aligned} L^{1111} &= 3, L^{1112} = 0, L^{1122} = 1, L^{1222} = 0, \\ L^{2222} &= 3 \end{aligned} \quad (\text{E.10})$$

We now want to calculate the spatially-dependent Fermi velocity and the gauge field to second order. Recall the expressions

$$\tilde{v}^{ij}(\mathbf{x}) = \sum_n \frac{2}{3t_0 a^2} l_n^i l_n^j \left(t_n(\mathbf{x}) - \frac{1}{2} l_n^k \partial_k t_n(\mathbf{x}) \right), \quad (\text{E.11})$$

$$A_i^s(\mathbf{x}) = \sum_n \frac{2}{3t_0 a^2} \epsilon_{ij} l_n^j \left(t_n(\mathbf{x}) - \frac{1}{2} l_n^k \partial_k t_n(\mathbf{x}) \right) \quad (\text{E.12})$$

Plugging in, we find

$$\tilde{v}^{ij}(\mathbf{x}) = \delta^{ij} - \frac{\beta}{4} L^{ijkl} u_{kl} \quad (\text{E.13})$$

$$\tilde{v}^{ij} = \delta^{ij} - \frac{\beta}{4} (u^{ij} + u^{ji} + \delta^{ij} u^{kk}) \quad (\text{E.14})$$

Furthermore, we find

$$A_i^s(\mathbf{x}) = \frac{\epsilon_{ij}}{a} \frac{\beta}{2} K^{ijkl} u_{kl} \quad (\text{E.15})$$

$$\mathbf{A}^s = \frac{\beta}{2a} \begin{pmatrix} u_{yy} - u_{xx} \\ u_{xy} + u_{yx} \end{pmatrix}. \quad (\text{E.16})$$

(E.14) and (E.16) agree with the results in [1]. However, the fact that the results coincide is non-trivial. We note that compared to [1] we have included the trigonal warping term in (E.2). We also have the additional derivative terms in (3.3) and (3.4). These additional derivative terms exactly cancel off the contribution from the trigonal warping. Moreover, the combination of the trigonal warping and the extra terms in (3.3) and (3.4) also eliminate the extra gauge potential $\tilde{\mathbf{A}}_a$ of Ref. [4]. The $\tilde{\mathbf{A}}_a$ term of Ref. [4], with the presence of ϵ_{ab} , is forbidden by the reflection symmetry, see [28] and [60] for more detailed arguments.

F Second-order calculation: exponential tunneling

We assume that each lattice site is displaced as

$$\mathbf{x} \rightarrow \mathbf{x} + \mathbf{u}(\mathbf{x}) \quad (\text{F.1})$$

Two lattice sites that were previously separated by \mathbf{l}_n will now be separated by

$$\mathbf{l}'_n = \mathbf{l}_n + \mathbf{u}(\mathbf{x} + \mathbf{l}_n) - \mathbf{u}(\mathbf{x}) \approx \mathbf{l}_n + (\mathbf{l}_n \cdot \nabla) \mathbf{u} + \frac{1}{2} (\mathbf{l}_n \cdot \nabla)^2 \mathbf{u} \quad (\text{F.2})$$

We now note that there are two small parameters in the problem. Defining $a \equiv |\mathbf{l}_n|$ and L as the total size of the system,

$$\frac{(\mathbf{l}_n \cdot \nabla) \mathbf{u}}{a} \sim \frac{\mathbf{u}}{L} \quad (\text{F.3})$$

$$\left(\frac{(\mathbf{l}_n \cdot \nabla) \mathbf{u}}{a}\right) \sim \left(\frac{\mathbf{u}}{L}\right)^2 \quad (\text{F.4})$$

$$\frac{(\mathbf{l}_n \cdot \nabla)^2 \mathbf{u}}{a} \sim \frac{\mathbf{u}}{L} \frac{a}{L} \quad (\text{F.5})$$

We assume that the two small parameters \mathbf{u}/L and a/L are of a similar order of smallness and expand to second-order in these small parameters. Expanding, we find after some algebra

$$\frac{|\mathbf{l}'_n| - a}{a} \approx \frac{l_n^i l_n^j u_{ij}}{a^2} + \frac{l_n^i l_n^j u_{ik} u_{jk}}{2a^2} - \frac{l_n^i l_n^j l_n^k l_n^m u_{ij} u_{km}}{2a^4} + \frac{l_n^i l_n^j l_n^k \partial_i u_{jk}}{2a^2} \quad (\text{F.6})$$

where we have defined

$$u_{ij} \equiv \partial_i u_j \quad (\text{F.7})$$

To second order

$$\left(\frac{|\mathbf{l}'_n| - a}{a}\right)^2 \approx \frac{l_n^i l_n^j l_n^k l_n^m u_{ij} u_{km}}{a^4} \quad (\text{F.8})$$

The hopping will depend on the distance between the sites.

$$t_n(\mathbf{x}) \approx t_0 \cdot \left[1 - \beta \frac{|\mathbf{l}'_n| - a}{a} + \kappa \left(\frac{|\mathbf{l}'_n| - a}{a}\right)^2 \right] \quad (\text{F.9})$$

where the coefficients β and κ are defined by

$$\beta = -\frac{a}{t_0} \frac{\partial t}{\partial r} \Big|_{r=a}, \quad \kappa = \frac{a^2}{2t_0} \frac{\partial^2 t}{\partial r^2} \Big|_{r=a} \quad (\text{F.10})$$

For the typical exponentially decaying hopping, which is a good approximation in both the case of real graphene and its photonic analogue, we have $t = t_0 e^{-\beta(r-a)/a}$ and hence $\kappa = \beta^2/2$. In addition to the matrices defined in the previous section, it will be useful to define the following matrices

$$\frac{1}{a^5} \sum_{n=1}^3 l_n^i l_n^j l_n^k l_n^l l_n^m = -\frac{3}{16} M^{ijklm}, \quad (\text{F.11})$$

$$\frac{1}{a^6} \sum_{n=1}^3 l_n^i l_n^j l_n^k l_n^l l_n^m l_n^o = \frac{3}{32} N^{ijklmo}. \quad (\text{F.12})$$

The matrices M and N are completely symmetric in all their indices and hence have 6 and 7 independent components respectively. All the entries of these matrices are integers. The independent entries are

$$\begin{aligned} M^{11111} &= 0, & M^{11112} &= -3, & M^{11122} &= 0, \\ M^{11222} &= -1, & M^{12222} &= 0, & M^{22222} &= 5 \end{aligned} \quad (\text{F.13})$$

and

$$\begin{aligned} N^{111111} &= 9, & N^{111112} &= 0, & N^{111122} &= 3, \\ N^{111222} &= 0, & N^{112222} &= 1, & N^{122222} &= 0, \\ N^{222222} &= 11. \end{aligned} \quad (\text{F.14})$$

We now want to calculate the spatially-dependent Fermi velocity and the gauge field to second order. Recall the expressions

$$\tilde{v}^{ij}(\mathbf{x}) = \sum_n \frac{2}{3t_0 a^2} l_n^i l_n^j \left(t_n(\mathbf{x}) - \frac{1}{2} l_n^k \partial_k t_n(\mathbf{x}) \right), \quad (\text{F.15})$$

$$A_i^s(\mathbf{x}) = \sum_n \frac{2}{3t_0 a^2} \epsilon_{ij} l_n^j \left(t_n(\mathbf{x}) - \frac{1}{2} l_n^k \partial_k t_n(\mathbf{x}) \right) \quad (\text{F.16})$$

Plugging in, we find

$$\tilde{v}^{ij}(\mathbf{x}) = \delta^{ij} - \beta \left(\frac{1}{4} L^{ijkl} u_{kl} + \frac{1}{8} L^{ijkl} u_{km} u_{lm} - \frac{1}{32} N^{ijklmo} u_{kl} u_{mo} \right) + \frac{\kappa}{16} N^{ijklmo} u_{kl} u_{mo} \quad (\text{F.17})$$

To first order in strain,

$$\tilde{v}^{ij} = \delta^{ij} - \frac{\beta}{4} (u^{ij} + u^{ji} + \delta^{ij} u^{kk}) \quad (\text{F.18})$$

Furthermore, we find

$$A_i^s(\mathbf{x}) = \frac{\epsilon_{ij}}{a} \left[-\beta \left(-\frac{1}{2} K^{jkl} u_{kl} - \frac{1}{4} K^{jkl} u_{km} u_{lm} + \frac{1}{16} M^{jklmo} u_{kl} u_{mo} \right) - \frac{\kappa}{8} M^{jklmo} u_{kl} u_{mo} \right] \quad (\text{F.19})$$

Again, if we work to first order in strain, we find

$$\mathbf{A}^s = \frac{\beta}{2a} \begin{pmatrix} u_{yy} - u_{xx} \\ u_{xy} + u_{yx} \end{pmatrix}. \quad (\text{F.20})$$

To this order, (F.18) and (F.20) agree with the results in [1]. However, we have calculated the higher-order corrections. For the strain profile (4.2) and setting $\kappa = \beta^2/2$ we find curvature

$$\mathcal{K} = -\frac{4}{a^2} \left(\beta \frac{au_B}{L} \right)^2 \quad (\text{F.21})$$

and magnetic field

$$B = \frac{4}{a^2} \beta \frac{au_B}{L} - \frac{4}{a^2} \left(\beta \frac{au_B}{L} \right)^2. \quad (\text{F.22})$$

References

- [1] F. de Juan, M. Sturla and M. A. H. Vozmediano, *Space dependent fermi velocity in strained graphene*, Physical Review Letters **108**(22) (2012), doi:[10.1103/physrevlett.108.227205](https://doi.org/10.1103/physrevlett.108.227205).
- [2] F. de Juan, J. L. Mañes and M. A. H. Vozmediano, *Gauge fields from strain in graphene*, Physical Review B **87**(16) (2013), doi:[10.1103/physrevb.87.165131](https://doi.org/10.1103/physrevb.87.165131).
- [3] M. Oliva-Leyva and G. G. Naumis, *Generalizing the fermi velocity of strained graphene from uniform to nonuniform strain*, Physics Letters A **379**(40), 2645 (2015), doi:<https://doi.org/10.1016/j.physleta.2015.05.039>.
- [4] M. A. Zubkov and G. E. Volovik, *Emergent gravity in graphene*, Journal of Physics: Conference Series **607**, 012020 (2015), doi:[10.1088/1742-6596/607/1/012020](https://doi.org/10.1088/1742-6596/607/1/012020).
- [5] M. Oliva-Leyva and C. Wang, *Low-energy theory for strained graphene: an approach up to second-order in the strain tensor*, Journal of Physics: Condensed Matter **29**(16), 165301 (2017), doi:[10.1088/1361-648x/aa62c9](https://doi.org/10.1088/1361-648x/aa62c9).
- [6] Z. V. Khaidukov and M. A. Zubkov, *Landau levels in graphene in the presence of emergent gravity*, The European Physical Journal B **89**(10), 213 (2016), doi:[10.1140/epjb/e2016-70182-7](https://doi.org/10.1140/epjb/e2016-70182-7).
- [7] B. Yang, *Dirac cone metric and the origin of the spin connections in monolayer graphene*, Phys. Rev. B **91**, 241403 (2015), doi:[10.1103/PhysRevB.91.241403](https://doi.org/10.1103/PhysRevB.91.241403).

- [8] A. Iorio and P. Pais, *Revisiting the gauge fields of strained graphene*, Phys. Rev. D **92**, 125005 (2015), doi:[10.1103/PhysRevD.92.125005](https://doi.org/10.1103/PhysRevD.92.125005).
- [9] E. Arias, A. R. Hernández and C. Lewenkopf, *Gauge fields in graphene with nonuniform elastic deformations: A quantum field theory approach*, Phys. Rev. B **92**, 245110 (2015), doi:[10.1103/PhysRevB.92.245110](https://doi.org/10.1103/PhysRevB.92.245110).
- [10] C. Si, Z. Sun and F. Liu, *Strain engineering of graphene: a review*, Nanoscale **8**, 3207 (2016), doi:[10.1039/C5NR07755A](https://doi.org/10.1039/C5NR07755A).
- [11] A. H. Castro Neto, F. Guinea, N. M. R. Peres, K. S. Novoselov and A. K. Geim, *The electronic properties of graphene*, Rev. Mod. Phys. **81**, 109 (2009), doi:[10.1103/RevModPhys.81.109](https://doi.org/10.1103/RevModPhys.81.109).
- [12] E. Fradkin, *Field theories of condensed matter physics*, Cambridge University Press (2013).
- [13] T. L. Linnik, *Effective hamiltonian of strained graphene*, Journal of Physics: Condensed Matter **24**(20), 205302 (2012), doi:[10.1088/0953-8984/24/20/205302](https://doi.org/10.1088/0953-8984/24/20/205302).
- [14] J. L. Mañes, *Symmetry-based approach to electron-phonon interactions in graphene*, Phys. Rev. B **76**, 045430 (2007), doi:[10.1103/PhysRevB.76.045430](https://doi.org/10.1103/PhysRevB.76.045430).
- [15] R. Winkler and U. Zülicke, *Invariant expansion for the trigonal band structure of graphene*, Phys. Rev. B **82**, 245313 (2010), doi:[10.1103/PhysRevB.82.245313](https://doi.org/10.1103/PhysRevB.82.245313).
- [16] F. Guinea, M. I. Katsnelson and A. K. Geim, *Energy gaps and a zero-field quantum hall effect in graphene by strain engineering*, Nature Physics **6**, 30 (2009).
- [17] M. Settnes, S. R. Power and A.-P. Jauho, *Pseudomagnetic fields and triaxial strain in graphene*, Phys. Rev. B **93**, 035456 (2016).
- [18] N. Levy, S. A. Burke, K. L. Meaker, M. Panlasigui, A. Zettl, F. Guinea, A. H. C. Neto and M. F. Crommie, *Strain-induced pseudo-magnetic fields greater than 300 tesla in graphene nanobubbles*, Science **329**(5991), 544 (2010), doi:[10.1126/science.1191700](https://doi.org/10.1126/science.1191700).
- [19] N.-C. Yeh, M.-L. Teague, S. Yeom, B. Standley, R.-P. Wu, D. Boyd and M. Bockrath, *Strain-induced pseudo-magnetic fields and charging effects on cvd-grown graphene*, Surface Science **605**(17), 1649 (2011), doi:<https://doi.org/10.1016/j.susc.2011.03.025>, Graphene Surfaces and Interfaces.
- [20] J. Lu, A. H. C. Neto and K. P. Loh, *Transforming moiré blisters into geometric graphene nanobubbles*, Nature Communications **3**, 823 (2012), Article.
- [21] S.-Y. Li, K.-K. Bai, L.-J. Yin, J.-B. Qiao, W.-X. Wang and L. He, *Observation of unconventional splitting of landau levels in strained graphene*, Phys. Rev. B **92**, 245302 (2015).
- [22] J.-D. Debus, M. Mendoza and H. J. Herrmann, *Shifted landau levels in curved graphene sheets*, Journal of Physics: Condensed Matter **30**(41), 415503 (2018), doi:[10.1088/1361-648x/aadecd](https://doi.org/10.1088/1361-648x/aadecd).
- [23] J. González, F. Guinea and M. Vozmediano, *The electronic spectrum of fullerenes from the dirac equation*, Nuclear Physics B **406**(3), 771 (1993), doi:[https://doi.org/10.1016/0550-3213\(93\)90009-E](https://doi.org/10.1016/0550-3213(93)90009-E).
- [24] E. Lantagne-Hurtubise, X.-X. Zhang and M. Franz, *Dispersive landau levels and valley currents in strained graphene nanoribbons* (2019), [1909.01442](https://arxiv.org/abs/1909.01442).
- [25] G. Salerno, T. Ozawa, H. M. Price and I. Carusotto, *How to directly observe landau levels in driven-dissipative strained honeycomb lattices*, 2D Materials **2**(3), 034015 (2015), doi:[10.1088/2053-1583/2/3/034015](https://doi.org/10.1088/2053-1583/2/3/034015).
- [26] E. V. Castro, A. Flachi, P. Ribeiro and V. Vitagliano, *Symmetry breaking and lattice kirigami*, Phys. Rev. Lett. **121**, 221601 (2018), doi:[10.1103/PhysRevLett.121.221601](https://doi.org/10.1103/PhysRevLett.121.221601).

- [27] A. Cortijo and M. A. Vozmediano, *Effects of topological defects and local curvature on the electronic properties of planar graphene*, Nuclear Physics B **763**(3), 293 (2007), doi:<https://doi.org/10.1016/j.nuclphysb.2006.10.031>.
- [28] J. L. Mañes, F. de Juan, M. Sturla and M. A. H. Vozmediano, *Generalized effective hamiltonian for graphene under nonuniform strain*, Phys. Rev. B **88**, 155405 (2013), doi:[10.1103/PhysRevB.88.155405](https://doi.org/10.1103/PhysRevB.88.155405).
- [29] M. R. Masir, D. Moldovan and F. Peeters, *Pseudo magnetic field in strained graphene: Revisited*, Solid State Communications **175-176**, 76 (2013), doi:<https://doi.org/10.1016/j.ssc.2013.04.001>, Special Issue: Graphene V: Recent Advances in Studies of Graphene and Graphene analogues.
- [30] N. Schine, A. Ryou, A. Gromov, A. Sommer and J. Simon, *Synthetic landau levels for photons*, Nature **534**, 671 (2016).
- [31] N. Schine, M. Chalupnik, T. Can, A. Gromov and J. Simon, *Electromagnetic and gravitational responses of photonic landau levels*, Nature **565**(7738), 173 (2019), doi:[10.1038/s41586-018-0817-4](https://doi.org/10.1038/s41586-018-0817-4).
- [32] R. A. Bertlmann, *Anomalies in Quantum Field Theory*, OUP Oxford, ISBN 0198507623 (2000).
- [33] R. M. Wald, *General relativity*, Chicago Univ. Press, Chicago, IL (1984).
- [34] S. Weinberg, *Gravitation and Cosmology: Principles and Applications of the General Theory of Relativity*, Wiley, New York, NY (1972).
- [35] T. Frankel, *The Geometry of Physics: An Introduction*, Cambridge University Press, 3 edn., doi:[10.1017/CBO9781139061377](https://doi.org/10.1017/CBO9781139061377) (2011).
- [36] A. Pnueli, *Spinors and scalars on riemann surfaces*, Journal of Physics A: Mathematical and General **27**(4), 1345 (1994), doi:[10.1088/0305-4470/27/4/028](https://doi.org/10.1088/0305-4470/27/4/028).
- [37] T. L. Hughes, R. G. Leigh and O. Parrikar, *Torsional anomalies, hall viscosity, and bulk-boundary correspondence in topological states*, Phys. Rev. D **88**, 025040 (2013), doi:[10.1103/PhysRevD.88.025040](https://doi.org/10.1103/PhysRevD.88.025040).
- [38] C. Hoyos, *Hall viscosity, topological states and effective theories*, International Journal of Modern Physics B **28**(15), 1430007 (2014), doi:[10.1142/S0217979214300072](https://doi.org/10.1142/S0217979214300072), <https://doi.org/10.1142/S0217979214300072>.
- [39] F. de Juan, A. Cortijo and M. A. Vozmediano, *Dislocations and torsion in graphene and related systems*, Nuclear Physics B **828**(3), 625 (2010), doi:<https://doi.org/10.1016/j.nuclphysb.2009.11.012>.
- [40] R. M. Ribeiro, V. M. Pereira, N. M. R. Peres, P. R. Briddon and A. H. C. Neto, *Strained graphene: tight-binding and density functional calculations*, New Journal of Physics **11**(11), 115002 (2009), doi:[10.1088/1367-2630/11/11/115002](https://doi.org/10.1088/1367-2630/11/11/115002).
- [41] S. Rachel, I. Göthel, D. P. Arovas and M. Vojta, *Strain-induced landau levels in arbitrary dimensions with an exact spectrum*, Phys. Rev. Lett. **117**, 266801 (2016), doi:[10.1103/PhysRevLett.117.266801](https://doi.org/10.1103/PhysRevLett.117.266801).
- [42] C. Poli, J. Arkininstall and H. Schomerus, *Degeneracy doubling and sublattice polarization in strain-induced pseudo-landau levels*, Phys. Rev. B **90**, 155418 (2014), doi:[10.1103/PhysRevB.90.155418](https://doi.org/10.1103/PhysRevB.90.155418).
- [43] J. K. Pachos, *Manifestations of topological effects in graphene*, Contemporary Physics **50**(2), 375 (2009), doi:[10.1080/00107510802650507](https://doi.org/10.1080/00107510802650507).
- [44] M. O. Goerbig, *Electronic properties of graphene in a strong magnetic field*, Rev. Mod. Phys. **83**, 1193 (2011), doi:[10.1103/RevModPhys.83.1193](https://doi.org/10.1103/RevModPhys.83.1193).
- [45] X. G. Wen and A. Zee, *Shift and spin vector: New topological quantum numbers for the hall fluids*, Phys. Rev. Lett. **69**, 953 (1992), doi:[10.1103/PhysRevLett.69.953](https://doi.org/10.1103/PhysRevLett.69.953).

- [46] Z. V. Khaidukov and M. A. Zubkov, *Landau levels in graphene in the presence of emergent gravity*, The European Physical Journal B **89**(10), 213 (2016), doi:[10.1140/epjb/e2016-70182-7](https://doi.org/10.1140/epjb/e2016-70182-7).
- [47] M. C. Rechtsman, Y. Plotnik, J. M. Zeuner, D. Song, Z. Chen, A. Szameit and M. Segev, *Topological creation and destruction of edge states in photonic graphene*, Phys. Rev. Lett. **111**, 103901 (2013), doi:[10.1103/PhysRevLett.111.103901](https://doi.org/10.1103/PhysRevLett.111.103901).
- [48] Y. Plotnik, M. C. Rechtsman, D. Song, M. Heinrich, J. M. Zeuner, S. Nolte, Y. Lumer, N. Malkova, J. Xu, A. Szameit, Z. Chen and M. Segev, *Observation of unconventional edge states in 'photonic graphene'*, Nature Materials **13**, 57 (2013), Article.
- [49] M. C. Rechtsman, J. M. Zeuner, A. Tünnermann, S. Nolte, M. Segev and A. Szameit, *Strain-induced pseudomagnetic field and photonic landau levels in dielectric structures*, Nature Photonics **7**, 153 (2012), Article.
- [50] M. C. Rechtsman, J. M. Zeuner, Y. Plotnik, Y. Lumer, D. Podolsky, F. Dreisow, S. Nolte, M. Segev and A. Szameit, *Photonic floquet topological insulators*, Nature **496**, 196 (2013).
- [51] B. Xie, H. Liu, H. Cheng, Z. Liu, S. Chen and J. Tian, *Acoustic topological transport and refraction in a kekulé lattice*, Phys. Rev. Applied **11**, 044086 (2019), doi:[10.1103/PhysRevApplied.11.044086](https://doi.org/10.1103/PhysRevApplied.11.044086).
- [52] P. Gao, D. Torrent, F. Cervera, P. San-Jose, J. Sanchez-Dehesa and J. Christensen, *Majorana-like zero modes in kekulé distorted sonic lattices* (2019), [1910.01956](https://arxiv.org/abs/1910.01956).
- [53] H. Abbaszadeh, A. Souslov, J. Paulose, H. Schomerus and V. Vitelli, *Sonic landau levels and synthetic gauge fields in mechanical metamaterials*, Phys. Rev. Lett. **119**, 195502 (2017), doi:[10.1103/PhysRevLett.119.195502](https://doi.org/10.1103/PhysRevLett.119.195502).
- [54] O. Boada, A. Celi, J. I. Latorre and M. Lewenstein, *Dirac equation for cold atoms in artificial curved spacetimes*, New Journal of Physics **13**(3), 035002 (2011), doi:[10.1088/1367-2630/13/3/035002](https://doi.org/10.1088/1367-2630/13/3/035002).
- [55] J. González and J. Herrero, *Graphene wormholes: A condensed matter illustration of dirac fermions in curved space*, Nuclear Physics B **825**(3), 426 (2010), doi:<https://doi.org/10.1016/j.nuclphysb.2009.09.028>.
- [56] S. Bonanos, *Capabilities of the Mathematica package Riemannian Geometry and Tensor Calculus*, pp. 174–182.
- [57] D. Z. Freedman and A. Van Proeyen, *Supergravity*, Cambridge Univ. Press, Cambridge, UK, ISBN 9781139368063, 9780521194013 (2012).
- [58] D. T. Son, *Is the composite fermion a dirac particle?*, Phys. Rev. X **5**, 031027 (2015), doi:[10.1103/PhysRevX.5.031027](https://doi.org/10.1103/PhysRevX.5.031027).
- [59] L. Balents, *General continuum model for twisted bilayer graphene and arbitrary smooth deformations*, SciPost Phys. **7**, 48 (2019), doi:[10.21468/SciPostPhys.7.4.048](https://doi.org/10.21468/SciPostPhys.7.4.048).
- [60] R. Winkler and U. Zülicke, *Invariant expansion for the trigonal band structure of graphene*, Phys. Rev. B **82**, 245313 (2010), doi:[10.1103/PhysRevB.82.245313](https://doi.org/10.1103/PhysRevB.82.245313).